JOURNAL OF COMPUTATIONAL PHYSICS **136,** 132–139 (1997)
ARTICLE NO. CP975751

Computations of Slowly Moving Shocks

Smadar Karni*,[1] and Sunčica Čanić†,[2]

*Temple University, Philadelphia, Pennsylvania 19122; and †Department of Mathematics, 400 Carver Hall, Iowa State University, Ames, Iowa 50011

Received September 9, 1996; revised April 17, 1997

Computations of slowly moving shocks by shock capturing schemes may generate oscillations that appear as a wavy tail attached to the shock front. These oscillations are generated already by first-order schemes, but become more pronounced in higher-order schemes due to their lower dissipation. We focus on two first-order schemes which seem to exhibit different behaviors: (i) the first-order upwind (UW) scheme which generates strong oscillations and (ii) the Lax–Friedrichs scheme which appears not to generate any disturbances at all. A key observation is that in the UW case, the numerical viscosity in the shock family vanishes inside the slow shock layer. Simple scaling arguments show that third-order effects on the solution may no longer be neglected. We derive the third-order modified equation for the UW scheme and regard the oscillatory solution as a traveling wave solution of the parabolic modified equation plus a small perturbation. We then look at the governing equation for the perturbation, which points to a plausible mechanism by which postshock oscillations are generated. It contains a third-order source term that becomes significant inside the shock layer, and a nonlinear coupling term which projects the perturbation on all characteristic fields, including those not associated with the shock family.

1. INTRODUCTION

Numerically captured shocks produce $O(1)$ errors inside the shock layer. Within the shock capturing framework, inaccuracies that are contained within the shock layer are regarded as acceptable, since this layer can be made arbitrarily narrow by using fine computational grids. This would be a satisfactory state of affairs if indeed the errors induced remained within the shock layer.

Computations of slowly moving shocks provide an example where such errors escape outside the shock layer and take the form of a persistent wavy tail. These are amplitude errors, not phase errors that are often considered less harmful. They may harm the computed solution even if eventually it converges to the correct limit. For example, postshock oscillations may significantly inhibit the convergence of transient solutions to steady state. They would definitely be harmful to calculations of shock sound interactions, where the amplitudes of interest are very small compared to the background flow.

The problem was first observed by Woodward and Colella [5] and further studied by Roberts [4]. More recently, two papers have proposed explanations for this peculiar phenomenon. Arora and Roe [1] noted that while initial shock data lie on the Hugoniot curve through, say, the left state, subsequent intermediate states inside the shock layer usually do not. Hence, solutions of subsequent Riemann problems generate a whole fan of wave, not only the shock wave itself. Jin and Liu [2] interpreted the phenomenon in the context of traveling wave solutions for the modified equation. They observed that slow captured shocks in gas dynamics admit (nonphysical) strong undershoots in the momentum profiles, and they suggest that unsteadiness in the momentum profile, and in particular in the momentum spike, is the cause for the oscillations.

The work presented here benefits from both of these papers. We remain within the framework of traveling waves presented in [2] which we believe provides a suitable context for understanding the phenomenon. We have adopted from [1] the use of phase diagrams and numerical orbits, a tool which we find very insightful. What makes this phenomenon difficult to analyze is that it is inherently nonlinear and occurs only in systems of equations; thus the simplest setup for studying it is the 2×2 case. We have focused on the isothermal Euler equations as one such example, and where appropriate we make comments about other systems. The arguments we put forward equally apply to larger systems.

Two facts have caught our eyes: (i) Phase space diagrams of computed propagating shocks (fast or slow) yield extremely clean and well-defined numerical orbits as soon as the shocks settle into their viscous profile [1]. (ii) For slow shocks in gas dynamics, the first-order upwind scheme (UW) generates very strong postshock oscillations while

[1] This work was conducted while the author was a visiting member at Courant Institute of Mathematical Sciences, New York University. Work supported by an NSF Postdoctoral Fellowship, DOE contract #DEFG0288ER25053, NSF grant DMS 94 96155 and ONR grant N00014-94-I-0525. Present address: Department of Mathematics, University of Michigan, Ann Arbor, MI 48109.

[2] Work supported by NSF grants DMS 94 03598 and DMS 96 25831, and by DOE contract #DEFG0294ER25220.

0021-9991/97 $25.00

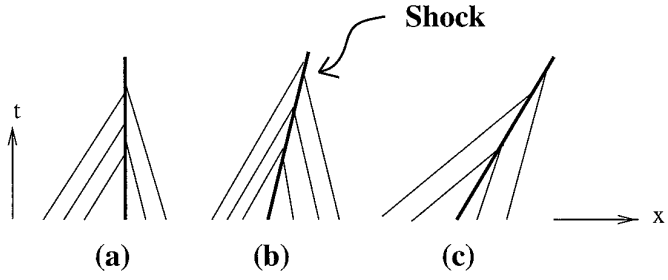

FIG. 1. (a) Stationary shock, (b) slowly moving shock, and (c) fast shock. Shock characteristics change sign across slow shock front.

in the Lax–Friedrichs (LxF) scheme, they are impossible to detect. In gas dynamics, both schemes generate solutions with deep undershoots in the momentum profiles [2]. Fact (i) seems to suggest that after a sufficiently long time, the discrete shock approaches a traveling wave, and this seems to support the traveling wave framework of [2]. While the theory in [2] explains the cause of the undershoots in the momentum profiles, it cannot account for the distinctively different behavior of the two schemes. We believe that this difference is at the heart of the mechanism responsible for generating postshock oscillations.

As in [1, 2], the emphasis in our work was not put on finding cures to the problem, but rather on uncovering the mechanisms responsible for this phenomenon. To a great extent, and this is also the conclusion of our work, the cure is known; namely, add more numerical dissipation. In fact, we show that employing an ''entropy fix'' may eliminate the oscillations. This, as always, comes at the expense of added diffusion and hence has its disadvantages. However, if one wishes to remain within the simple shock capturing framework, this may be a price one must learn to live with.

2. SLOW SHOCKS

Slow shocks are characterized by a sign change in the shock characteristic across the shock front [1, 4, 5]. This is certainly the case for stationary shocks, and so it will remain true if the shock is moving sufficiently slowly (see Fig. 1). Another characterization of slow shocks is that they take many steps to cross one computational cell. It is worth noting [1] that any shock may appear to be slow if viewed from a frame of reference moving almost at the shock speed. This boils down to superimposing a drift velocity on the data. Thus, there is no connection between the apparent speed of the shock and its strength. In the computations presented in this work, all shocks, fast or slow, are of identical strength. This eliminates one parameter from the problem. In computations of slowly moving shocks, different schemes generate oscillations of different amplitudes, and some may not generate oscillations at all. However, the wavelength of the oscillations with respect to the grid, i.e., the number of grid points per period of oscillation, is independent of the scheme and is related to the ratio of the respective cross family characteristic speed, say $|\lambda|_1$, to the shock speed, s [1, 2, 5].

In our computations and analysis, we have used the isothermal Euler equations

$$W_t + F(W)_x = 0 \tag{1a}$$

$$W = \begin{pmatrix} \rho \\ \rho u \end{pmatrix}, \quad F(W) = \begin{pmatrix} \rho u \\ \rho u^2 + \rho c^2 \end{pmatrix}. \tag{1b}$$

Here ρ is the density, u is the velocity, and c is the constant speed of sound ($c^2 = \gamma RT$ is constant in the isothermal case) and is taken to be 1. We use $A = \partial F(W)/\partial W$ to denote the Jacobian matrix, R the matrix of right eigenvectors, and Λ the diagonal matrix of the corresponding real eigenvalues. For the isothermal Euler equations

$$A = \begin{pmatrix} 0 & 1 \\ u^2 - c^2 & 2u \end{pmatrix}, \quad R = \begin{pmatrix} 1 & 1 \\ u - c & u + c \end{pmatrix}, \quad \Lambda = \begin{pmatrix} u - c & 0 \\ 0 & u + c \end{pmatrix}. \tag{1c}$$

Figure 2 shows computations of slowly moving shocks, performed by the LxF scheme (Fig. 2a) and the UW scheme (Fig. 2b). Initial data correspond to a slow shock moving to the right with speed $s = 0.05$, $W_R = (\rho_R, u_R) = (1, -2+ s)$, and $W_L = (\rho_L, u_L) = (4, -0.5 + s)$. For these data, $|\lambda_1|_L/s = |u_L - 1|/s \approx 30$. We see that in both calculations, the momentum profile develops a very strong undershoot. As pointed out in [2], this undershoot is nonphysical, and is due to the effect of numerical viscosity in the continuity equation. The other striking fact is that the shock computed by the UW scheme (Fig. 2b) has a long wavy tail attached to it. The shock computed by the LxF scheme (Fig. 2a) appears to be oscillation-free. Zooming into the oscillatory tail of the UW calculation (Fig. 3), we count roughly 30 grid points per period of oscillation, in agreement with the ratio $|\lambda_1(W_L)|/s$ [5].

3. NUMERICAL ORBITS AND TRAVELING WAVES

A very useful tool in understanding numerical shock profiles is numerical phase diagrams [1]. The discrete profile of a captured shock spreads over several grid points, which may be collected and plotted in phase space $(\rho, \rho u)$. One solution profile does not provide enough data points to plot an informative phase diagram. The points ahead of (behind) the shock collapse onto a single point in phase

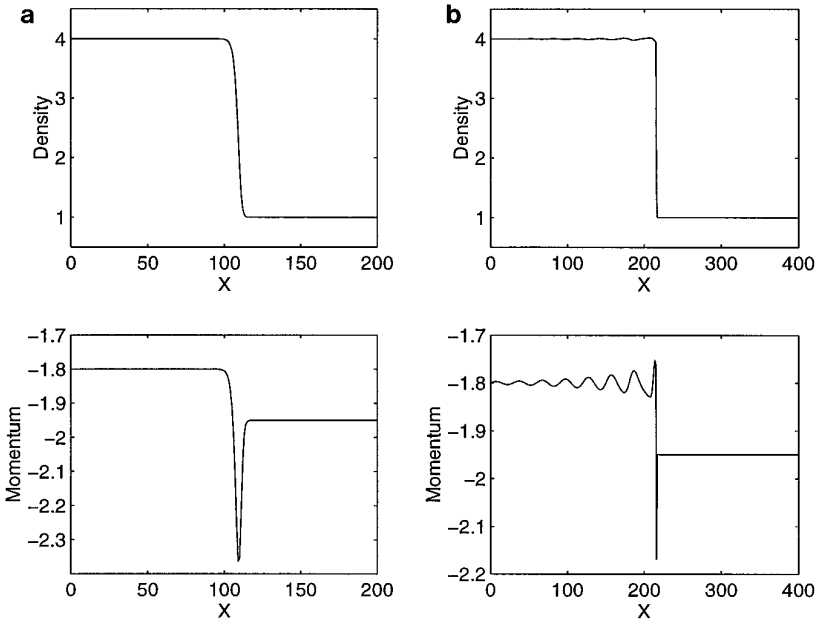

FIG. 2. Slowly moving shock by (a) LxF and (b) upwind schemes.

space, W_R (W_L), and the discrete profile may contain as few as 2–4 data points which is not enough to resolve a numerical orbit. Using many different discrete shock profiles of a propagating shock at many different times t_1, t_2, ..., t_n allows one to resolve the numerical orbit and provides useful information about the microscopic structure of the shock. As observed in [1], perfect shock data take some time to settle into a discrete viscous-like profile. However, once they do, discrete shock profiles maintain their structure very faithfully at all later times and generate extremely well-defined numerical orbits. Figure 4a shows the numerical orbit for a UW computation. Data are the same as in Fig. 2, except that this time the shock is fast ($s = 1.5$). The phase diagrams were generated from hundreds of discrete solution profiles at different time steps (omitting the first couple of hundred). The solution appears to be following very accurately the same numerical orbit.

A first candidate for what this orbit might represent is a traveling wave solution to the *modified equation*

$$W_t + F(W)_x = \varepsilon(D(W)W_x)_x, \tag{2}$$

where the right-hand side of (2) is the effective numerical viscosity of the scheme, and ε is the mesh spacing. For the UW and LxF schemes, $\varepsilon = \Delta t$ and the numerical viscosities are the leading order terms in the scheme truncation error, given respectively by

$$\begin{aligned} D(W)^{\mathrm{UW}} &= \frac{1}{2}\left(|A(W)|\frac{\Delta x}{\Delta t} - A^2(W)\right) \\ D(W)^{\mathrm{LxF}} &= \frac{1}{2}\left(\left(\frac{\Delta x}{\Delta t}\right)^2 I - A^2(W)\right). \end{aligned} \tag{3}$$

The validity of this conjecture can be tested. Substitute into (2) a traveling wave solution

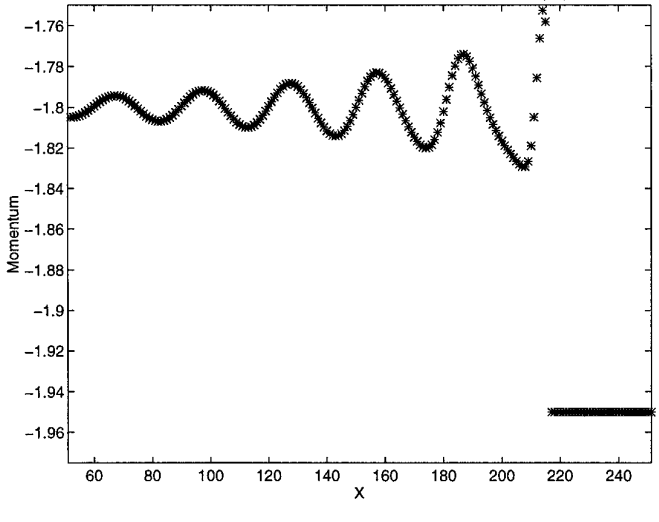

FIG. 3. Slowly moving shock by the UW scheme, $S = 0.05$: Zoom.

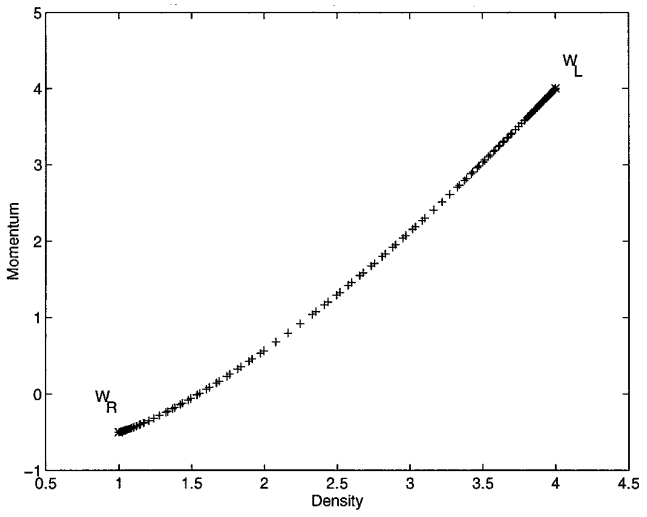

FIG. 4a. Numerical orbit of a fast shock ($S = 1.5$) by the upwind scheme.

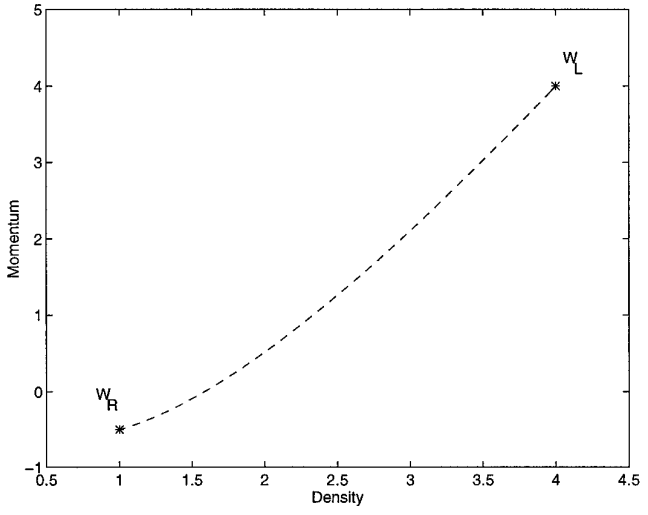

FIG. 4b. Traveling wave orbit of a fast shock ($S = 1.5$) by the upwind scheme.

$$W(x,t) = W(\xi), \quad \xi = \frac{x - st}{\varepsilon}$$
$$W(x \to \pm\infty, t) \to W_{\mathrm{L,R}} \tag{4}$$
$$W'(x \to \pm\infty, t) \to 0.$$

The parameter ε scales out and Eq. (2) becomes the ODE

$$-sW' + F'(W) = (D(W)W')'.$$

Integrating once over $(-\infty, \xi)$ we get the nonlinear dynamical system

$$W' = D^{-1}(W)(-s(W - W_{\mathrm{L}}) + F(W) - F_{\mathrm{L}}) \tag{5}$$

with rest points at W_{L} (saddle) and W_{R} (repeller). Equation (5) is nonlinear and in general cannot be integrated exactly. But it can be integrated numerically to give what we shall call the "theoretical" traveling wave solution. Figure 4b shows the traveling wave solution for the UW scheme for the same shock data as in Fig. 4a (LxF generates very similar results). For convenient comparison, the numerical orbit of the PDE solution and the traveling wave solution of the ODE are superimposed in Fig. 4c. The orbits are in very good agreement, good enough to say that the discrete PDE solution represents a traveling wave of (5). The close agreement between the numerical and theoretical orbits establishes that the traveling wave solution for the modified equation is indeed an appropriate framework for interpreting discrete propagating shocks. Also shown in Fig. 4c are the eigenvectors at the left and right states. Note that as theory predicts, the orbits leave the state W_{L} in a direction tangent to the shock family eigenvector r_2.

We now repeat these computations for the slowly moving shock example of Fig. 2. Figure 5 shows the numerical orbit and the traveling wave solution corresponding to the LxF scheme. The agreement between the two curves is very good in this case too. Both curves are tangent to the shock eigenvector $r_2(W_{\mathrm{L}})$ at the left state W_{L}. As in Fig. 2, we observe the fact that the momentum profile is nonmonotone and admits a strong undershoot. Figure 6 shows the numerical orbit and the traveling wave solution corre-

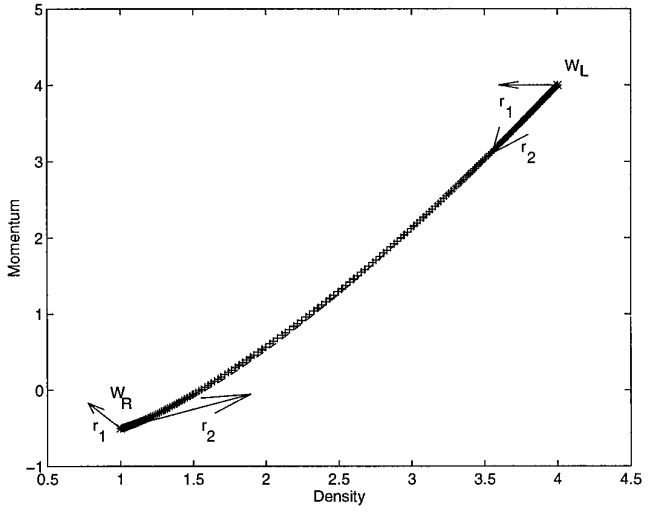

FIG. 4c. Traveling wave and numerical orbit of a fast shock ($S = 1.5$) by the upwind scheme. Also shown are the eigenvectors at the left and right states.

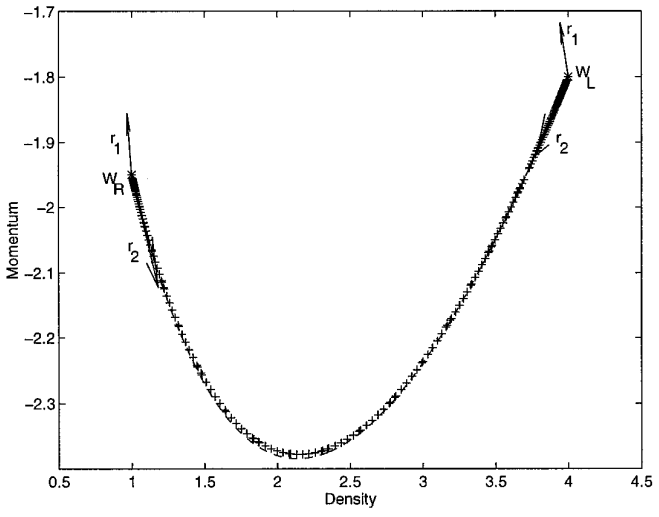

FIG. 5. Numerical and traveling wave orbits of a slow shock ($S = 0.05$) by the LxF scheme.

sponding to the UW scheme. In this case, the numerical orbit and the traveling wave solution give two different curves. Also note that the traveling wave orbit at W_L is tangent to the shock eigenvector $r_2(W_L)$, but the numerical orbit is tangential to the cross eigenvector $r_1(W_L)$. In fact, the entire oscillatory tail projects onto the cross family eigenvector $r_1(W_L)$, which appears as a dense set of data points near W_L in Fig. 6. The fact that the oscillations lie in the cross characteristic field has been observed before by other means [1, 2, 4]. In addition to the oscillations, we also note that the solution profile itself is modified and no longer agrees with the theoretical traveling wave solution of the parabolic PDE (2). Recall that this is the case where postshock oscillations are generated (see Fig. 1).

The difference in behavior between the two schemes is quite striking and calls for closer examination of the respective modified equations. Inspecting the numerical viscosities of the respective schemes suggests that the generation of the postshock oscillations may simply be a manifestation of an entropy violation due to vanishing dissipation, which is not dissimilar to several other situations where schemes fail exactly for that reason [3].

The eigenvalue associated with a slowly moving traveling wave, like slowly moving shocks, change sign across the wave front. For a right moving slow traveling wave, the eigenvalue behind the wave is positive, $\lambda_L > 0$, and that ahead of the wave is negative, $\lambda_R < 0$. It follows that somewhere inside the traveling wave profile, the eigenvalue changes sign, and in some neighborhood becomes very small. For the LxF viscosity, D^{LxF}, even when the eigenvalue vanishes viscosity is still finite due to the presence of the term $(\Delta x/\Delta t)^2$. For the UW scheme the situation is different. The dissipation in the shock family vanishes, D^{UW} becomes singular, and it is clear from Fig. 6 that the parabolic modified equation (2) is not a good model anymore. Indeed, the parabolic modified equation is valid only as long as higher-order terms in the scheme truncation errors are negligible. However, when $D(W)$ becomes small enough, the next term in the modified equation kicks in. This can be seen from the following simple scaling arguments.

4. SCALING ARGUMENTS

As a model for the modified equation up to third-order terms, consider Burger's equation with linear diffusion and linear dispersion

$$U_t + UU_x = \varepsilon D U_{xx} + \varepsilon^2 B U_{xxx}, \tag{6}$$

where ε is the mesh size. For smooth solutions, all the derivatives are $O(1)$ and the truncation error terms on the right-hand side (RHS) of (6) scale naturally with ε. By contrast, traveling wave solutions have the form $U(x, t) = U(x - st)/\varepsilon)$, and ε scales out of the problem. Hence for all purposes ε may be taken as 1. The modified equation remains asymptotically valid for *weak* traveling waves. The small parameter which provides the scale for the problem is the strength of the wave δ. Consider a weak traveling wave of the form

$$U(x, t) = U_0 + \delta U_1(\delta^p \xi), \quad \xi = x - st, \tag{7}$$

where U_0 is the linearized solution, $\delta \ll 1$ is the wave

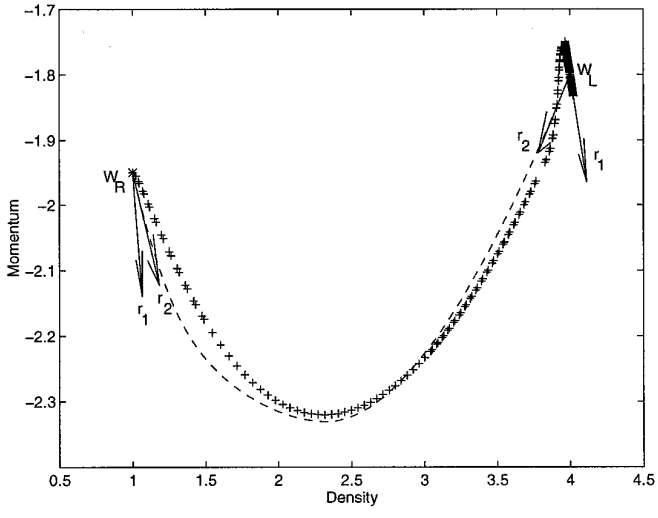

FIG. 6. Numerical and traveling wave orbits of a slow shock ($S = 0.05$) by the UW scheme.

amplitude, and δ^p is the scale of the solution for some p yet to be determined. Substituting into (6) we get

$$-s\delta^{p+1}U_1' + (U_0 + \delta U_1)\delta^{p+1}U_1' = D\delta^{2p+1}U_1'' + B\delta^{3p+1}U_1'''. \tag{8}$$

If both D and B are $O(1)$, the terms in the above equation would balance as

$$\begin{aligned} &\delta^{p+1}(-s + U_0)U_1' = 0 && \to U_0 = s \\ &\delta^{p+2}U_1U_1' + D\delta^{2p+1}U_1'' = 0 \to \\ &p + 2 = 2p + 1 && \to p = 1 \\ &B\delta^{3p+1}U_1''' = O(\delta^4) && \to \textit{negligible.} \end{aligned} \tag{9}$$

However, if the diffusion coefficient D is sufficiently small, then the diffusion and dispersion terms become comparable in magnitude. Assume that $D = d\delta^q$ for some q to be determined, with $d = O(1)$ and $B = O(1)$; then balancing the terms in Eq. (6) gives

$$\begin{aligned} &\delta^{p+1}(-s + U_0)U_1' = 0 && \to U_0 = s \\ &\delta^{p+2}U_1U_1' + d\delta^{2p+q+1}U_1'' = B\delta^{3p+1}U_1''' \to \\ &p + 2 = 2p + q + 1 = 3p + 1 && \to p = q = \tfrac{1}{2}, \end{aligned} \tag{10}$$

implying that as soon as $D = O(\sqrt{\delta})$, all three terms are of the same order of magnitude. This makes perfect sense. The nonlinearity causes the wave to steepen (scales like $O(\sqrt{\delta})$ rather than $O(\delta)$), and because the diffusion is weak, dispersion is needed for the wave to maintain a quasi-steady profile.

In the problem of slowly moving shocks, the diffusion (also dispersion) is nonlinear. Based on the above arguments the solution scales differently depending on the flow regime. Wherever $D(W) = O(1)$, third-order effects are negligible. Near an eigenvalue sign change inside a slow shock layer, diffusion becomes so small that third-order effects become of equal importance. We note that an eigenvalue sign change always implies small diffusion in some region. But it is possible to have small diffusion even without an eigenvalue sign change. For third-order effects to kick in, it is enough that diffusion is small compared with some measure of the wave strength. The p-system, for example, admits only fast shocks in the sense that eigenvalues never change sign across a shock front. Nevertheless, postshock oscillations may be observed [1]. In the example presented in [1], there is no eigenvalue sign change across the shock, but its magnitude is very small at the foot of the shock ($\lambda_2(W_R) = \sqrt{2/V_R^3} = 0.00388$), possibly small enough (compared with the shock strength) for a third-order effect to appear.

4.1. *Entropy Fix "Cure"*

The above analysis indicates that postshock oscillations may be eliminated by not allowing the diffusion in the shock family to become too small. It is easy to see why the common practice of increasing numerical viscosity helps in removing postshock oscillations. It helps to keep the third-order terms out of the problem. We have tried to use an entropy fix approach to remove the oscillations.

The numerical flux formula for the UW is

$$F_{j+1/2} = \frac{1}{2}(F_j + F_{j+1}) + \frac{1}{2}\sum_{k=1}^{n} \alpha_k|\lambda_k|r_k$$

and we replace $|\lambda_k|$ by $\max(|\lambda_k|, \delta)$, where δ is some measure of the wave strength. Using the shock wave amplitude $\delta = |U_R - U_L|$ completely eliminates the oscillations but at the same time introduces unnecessarily large amounts of dissipation. As a "local" measure of the wave strength, we use $|u_{j+1} - u_j|$. For no good reason other than the scaling suggested in the previous section, we have used a variable fix

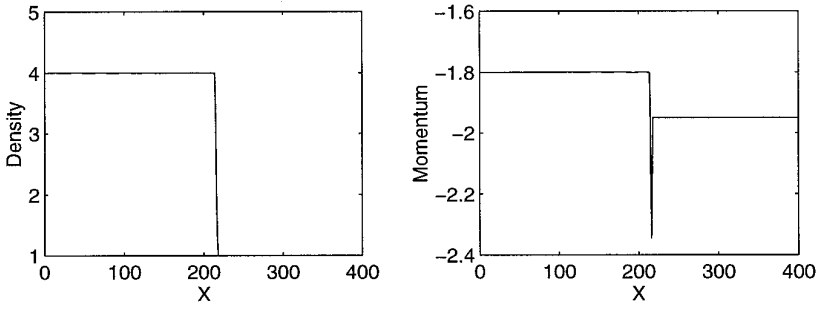

FIG. 7. Slow shock ($S = 0.05$) by upwind scheme with entropy fix.

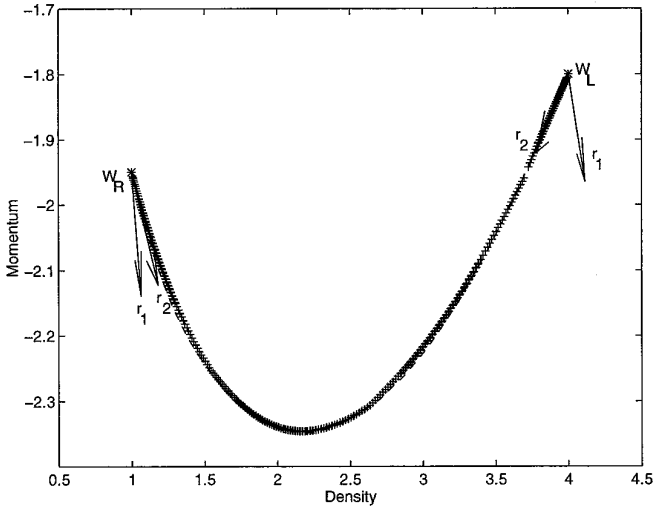

FIG. 8. Numerical and traveling wave orbits of a slow shock ($S = 0.05$) by the UW scheme with entropy fix.

$$\delta_{j+1/2} = \sqrt{|u_{j+1} - u_j|}.$$

Limiting the diffusion from below in this manner, we observe that the oscillations have pretty much disappeared (Fig. 7). We also observe (Fig. 8) that the numerical and traveling wave orbits that were distinctively different in Fig. 6 now practically coincide. We wish to stress that the above entropy fix is not proposed here as a practical way of curing the problem, since it may require unacceptably large amounts of dissipation. This particular form of entropy fix is expensive (due to square root operation) and was used following the asymptotic scaling arguments of Section 4. The entropy fix example is presented primarily as numerical evidence to the validity of the theory we are putting forward. It is worth noting, though, that the fixed UW scheme keeps a *very* narrow shock profile, much narrower than the LxF scheme (compare with Fig. 2a).

5. THIRD-ORDER MODIFIED EQUATION AND LINEARIZATION

In this section we derive the third-order modified equation for the upwind scheme. Assuming that the solution is a small perturbation to a traveling wave solution of (2), we linearize the modified equation about a traveling wave solution and obtain the governing equation for the perturbation. The purpose of this exercise is to point to certain terms that are present in the perturbation equation, terms which we believe play an important role in the problem: (i) a source-like term inside the shock layer and (ii) a nonlinear coupling term between the wave fields.

The modified equation for the UW scheme up to third-order terms is

$$W_t + F(W)_x = \frac{\Delta t}{2}\left((|A(W)|\frac{\Delta x}{\Delta t}W_x)_x - W_{tt}\right) - \frac{\Delta t^2}{6}\left(\left(\frac{\Delta x}{\Delta t}\right)^2 F(W)_{xxx} + W_{ttt}\right). \tag{11}$$

By time differentiating (11), time derivatives may be replaced by space derivatives (up to second order in the mesh $(\Delta x, \Delta t)$). W_{tt} is approximated up to first order in the mesh, W_{ttt} up to zero order, to give

$$W_t + F(W)_x = \Delta t(D(W)W_x)_x + \Delta t^2 S(W)_x, \tag{12a}$$

where

$$D(W) = \frac{1}{2}\left(|A|\frac{\Delta x}{\Delta t} - A^2\right)$$

$$S(W) = -\frac{1}{3}A(A^2W_x)_x + \frac{\lambda}{4}(A(|A|W_x)_x + |A|(AW_x)_x) - \frac{\lambda}{4}(|A|_tW_x) + \frac{1}{12}(A_tAW_x) - \frac{\lambda^2}{6}(AW_x)_x \tag{12b}$$

and $\lambda = \Delta x/\Delta t$ denotes the mesh ratio. The complexity of the above expression is quite off-putting, so we lump all the terms together and denote them by $S(W)$. Scaling arguments may be used to simplify (12b).

We write the solution W as a sum of a traveling wave solution to (2), $\bar{\mathscr{V}}$, plus a perturbation, $\mathscr{W}$,

$$W = \bar{\mathscr{V}} + \mathscr{W}.$$

With the assumption $\mathscr{W} \ll \bar{\mathscr{V}}$ we linearize Eq. (12) about the traveling wave profile

$$(\bar{\mathscr{V}} + \mathscr{W})_t + (F(\bar{\mathscr{V}}) + A(\bar{\mathscr{V}})\mathscr{W})_x = \Delta t\left(\left(D(\bar{\mathscr{V}}) + \frac{\partial D}{\partial W}(\bar{\mathscr{V}})\mathscr{W}\right)(\bar{\mathscr{V}} + \mathscr{W})_x\right)_x + \Delta t^2 S(\bar{\mathscr{V}})_x. \tag{13}$$

The traveling wave solution $\bar{\mathscr{V}}$ is assumed to satisfy

$$\bar{\mathscr{V}}_t + F(\bar{\mathscr{V}})_x = \Delta t(D(\bar{\mathscr{V}})\bar{\mathscr{V}}_x)_x; \tag{14}$$

hence it follows from (13) that the perturbation, $\mathscr{W}$, satisfies

$$\mathscr{W}_t + (A(\bar{\mathscr{V}})\mathscr{W})_x = \Delta t(D(\bar{\mathscr{V}})\mathscr{W}_x)_x + \Delta t\left(\left(\frac{\partial D}{\partial W}(\bar{\mathscr{V}})\mathscr{W}\right)\bar{\mathscr{V}}_x\right)_x + \Delta t^2 S(\bar{\mathscr{V}})_x. \tag{15}$$

Note that the term $((\partial D/\partial W)(\overline{\mathscr{V}})\mathscr{W})\overline{\mathscr{V}}_x$ on the right-hand side of (15) is linear in $\mathscr{W}$ and can be recast as

$$\left(\frac{\partial D}{\partial W}(\overline{\mathscr{V}})\mathscr{W}\right)\overline{\mathscr{V}}_x$$

$$= \begin{pmatrix} \dfrac{\partial D_{11}}{\partial u_1}\mathscr{W}_1 + \dfrac{\partial D_{11}}{\partial u_2}\mathscr{W}_2 & \dfrac{\partial D_{12}}{\partial u_1}\mathscr{W}_1 + \dfrac{\partial D_{12}}{\partial u_2}\mathscr{W}_2 \\ \dfrac{\partial D_{21}}{\partial u_1}\mathscr{W}_1 + \dfrac{\partial D_{21}}{\partial u_2}\mathscr{W}_2 & \dfrac{\partial D_{22}}{\partial u_1}\mathscr{W}_1 + \dfrac{\partial D_{22}}{\partial u_2}\mathscr{W}_2 \end{pmatrix} \begin{pmatrix} (\overline{\mathscr{V}}_1)_x \\ (\overline{\mathscr{V}}_2)_x \end{pmatrix}$$

$$\equiv B(\overline{\mathscr{V}}) \begin{pmatrix} \mathscr{W}_1 \\ \mathscr{W}_2 \end{pmatrix}$$

where $B(\overline{\mathscr{V}})$ is given by

$$= \begin{pmatrix} \dfrac{\partial D_{11}}{\partial u_1}(\overline{\mathscr{V}}_1)_x + \dfrac{\partial D_{12}}{\partial u_1}(\overline{\mathscr{V}}_2)_x & \dfrac{\partial D_{11}}{\partial u_2}(\overline{\mathscr{V}}_1)_x + \dfrac{\partial D_{12}}{\partial u_2}(\overline{\mathscr{V}}_2)_x \\ \dfrac{\partial D_{21}}{\partial u_1}(\overline{\mathscr{V}}_1)_x + \dfrac{\partial D_{22}}{\partial u_1}(\overline{\mathscr{V}}_2)_x & \dfrac{\partial D_{21}}{\partial u_2}(\overline{\mathscr{V}}_1)_x + \dfrac{\partial D_{22}}{\partial u_2}(\overline{\mathscr{V}}_2)_x \end{pmatrix}.$$

The equation for the perturbation, $\mathscr{W}$, becomes

$$\begin{aligned} &\mathscr{W}_t + ((A(\overline{\mathscr{V}}) - \Delta t B(\overline{\mathscr{V}}))\mathscr{W})_x \\ &\quad = \Delta t(D(\overline{\mathscr{V}})\mathscr{W}_x)_x + \Delta t^2 S(\overline{\mathscr{V}})_x. \end{aligned} \tag{17}$$

All the statements below are based on a careful numerical examination of the examples presented in this paper. They cannot be justified as general truth but we believe that, other than exceptions to the rule, they hold.

We make the following observations:

• $S(\overline{\mathscr{V}})$ is a source term that is nonzero only inside the shock layer. It is generally negligible in magnitude compared with the diffusion term, but becomes of equal magnitude in the narrow region where $D(\overline{\mathscr{V}})$ is small.

• $B(\overline{\mathscr{V}})$ is nonzero only inside the shock layer. Its significance is that it does *not* commute with the Jacobian matrix $A(\overline{\mathscr{V}})$ (we have checked numerically the eigenvectors of $A(\overline{\mathscr{V}})$ and $B(\overline{\mathscr{V}})$ across the traveling wave profile), and hence represents a nonlinear coupling term between the wave systems. We have also checked numerically the eigenvalues of the matrix $(A(\overline{\mathscr{V}}) - \Delta t B(\overline{\mathscr{V}}))$ across the traveling wave profile and they remain real.

• Both $S(\overline{\mathscr{V}})$ and $B(\overline{\mathscr{V}})$ move with the shock speed s.

$S(\overline{\mathscr{V}})$ generates perturbations, which, due to $B(\overline{\mathscr{V}})$, get projected onto all (here only two) characteristic fields.

• The projection onto the shock family gets swallowed into the shock and modifies its profile. This is why in Fig. 3b the numerical orbit is very different from the traveling wave solution.

• The projection onto the other family moves away with the corresponding characteristic speed and results in the oscillations that can be observed behind the shock.

The mechanism described above refines some of the observations made in [2], regarding the connection between traveling wave solutions to the modified equation and postshock oscillations. It points to a possible cause responsible for introducing unsteadiness into the slow shock profile, and can explain the puzzling different behavior of the UW and LxF schemes. While the momentum undershoot in the shock profile is an obvious numerical artifact, it is not more of an artifact than any $O(1)$ errors inside the shock layer. Furthermore, spiky momentum profiles may have an unsteady nature (UW) or an effectively steady nature (LxF, UW with entropy fix). What appears to be more significant is the fact that when dissipation in the shock field vanishes, the modified equation ceases to be a good model, and one needs to go (at least) one order higher in the modified equation and take into account third-order perturbations. When this happens, the traveling wave profiles steepen and become practically vertical (this, incidentally, is easiest to see in the density profile). Equation (17) identifies a source-like term for the perturbations, a nonlinear coupling between the fields, and a means by which the perturbations subsequently propagate.

ACKNOWLEDGMENTS

The authors thank Remi Abgrall, James Glimm, Jonathan Goodman, Jian-Guo Liu, Esteban Tabak, and Anders Szepessy for eye-opening conversations which helped the pieces of the puzzle drop into place. They may or may not recognize their contribution to this work, but they are gratefully acknowledged all the same.

REFERENCES

1. M. Arora and P. L. Roe, On post-shock oscillations due to shock capturing schemes in unsteady flows, *J. Comput. Phys.* **130,** 25 (1997).
2. S. Jin and J.-G. Liu, The effects of numerical viscosities. I. Slowly moving shocks, *J. Comput. Phys.* **126,** 373 (1996).
3. J. J. Quirk, A contribution to the great Riemann Solver debate, *Int. J. Numer. Methods Fluids* **18,** 555 (1994).
4. T. W. Roberts, The behaviour of flux difference schemes near slowly moving shock waves, *J. Comput. Phys.* **90,** (1990).
5. P. Woodward and P. Colella, The numerical simulation of two-dimensional fluid flow with strong shocks, *J. Comput. Phys.* **54,** 115 (1984).